

# Exploring the Rules for Selective Deposition: Interactions of Model Polyamines on Acid and Oligoethylene Oxide Surfaces

Xueping Jiang,<sup>†</sup> Christine Ortiz,<sup>‡</sup> and Paula T. Hammond<sup>\*,†</sup>

Departments of Chemical Engineering and Materials Science and Engineering,  
Massachusetts Institute of Technology, 25 Ames Street, 66-350,  
Cambridge, Massachusetts 02139-4307

Received June 5, 2001. In Final Form: September 4, 2001

New results using chemical force microscopy examine the relationships between polyions and both charged acid surface groups (COOH) and neutral oligoethylene oxide (EG) functionalized surfaces. Although poly(ethylene oxide) (PEO) and its derivatives have been known to resist protein deposition, our data indicate that certain hydrophobic polyelectrolytes, including polyallylamine hydrochloride (PAH), are actually attracted to the EG surface under certain pH conditions. Polymer surface modified colloidal particles were used as force probes to examine the interactions of polyamines with hydrophilic backbones, such as linear polyethyleneimine, and those with hydrophobic backbones, such as PAH, on alkanethiol monolayers. The adsorption and force curves of these two model polyamines with COOH and EG surfaces at a range of pH values is discussed. It is thought that the behavior observed is related to conformational differences between the hydrophobic and hydrophilic polymers at certain degrees of ionization. The differences in adsorption behavior of these and other polymers can be used as a tool to effectively control the region of film deposition. In general, these studies of synthetic polyamines have implications in understanding the nature of PEO-functionalized bioinert surfaces and the interactions of more complex polyelectrolytes such as proteins with EO-functionalized surfaces.

## 1. Introduction

Among the most critical functional groups found in both natural and synthetic polyelectrolytes are acid and amino groups. These functionalities undergo a balance of electrostatics and hydrogen bonding with each other that can result in adhesion and complexation that varies in strength as a function of pH and ionic strength. Of equal significance is the neutral, water-soluble polymer, poly(ethylene oxide) (PEO) and its oligomers, which are known to stabilize colloidal dispersions, act as antifouling agents on membranes,<sup>1</sup> and resist the adsorption of proteins and ultimately prevent the growth of cells on surfaces.<sup>2</sup> The molecular origin of the unique properties of PEO has been attributed to repulsive intermolecular interactions that outweigh other noncovalent attractive interactions. These repulsive interactions are thought to include enhanced steric repulsion due to a large affinity between the PEO repeat unit and water<sup>3–5</sup> which leads to increased excluded volume and osmotic pressure and enthalpic penalties for disruption of the helical backbone that PEO forms upon H-bonding with water.<sup>6</sup> Additional repulsive forces have also been recently attributed to an electrostatic double layer force due to an induced surface charge at the interface between the electrolyte and insulating PEO region in the presence of another charged surface nearby (e.g., pro-

teins).<sup>7</sup> Even for surfaces with short oligoethylene oxide self-assembling monolayers (SAMs), long-range repulsive forces are observed which are able to resist proteins<sup>8–11</sup> even though there are no steric interactions (which are solely associated with long polymer chains). It has been suggested that this phenomenon is due to the fact that the oligoethylene oxide layer acts as a template for the formation of an ordered water layer at the surface leading to repulsive hydration forces,<sup>12</sup> in addition to possible induced electrostatic double layer<sup>13,14</sup> and enthalpic repulsion components similar to that for PEO.

We have found that the above interactions which are critical to the control of protein deposition and cell growth on surfaces are also key to controlling the deposition of common synthetic polyelectrolytes and other charged species onto surfaces. Polyelectrolytes, like proteins, are generally prevented from deposition on oligoethylene oxide and PEO-functionalized surfaces. In this case, additional steric and electrostatic interactions may be imparted by the adsorbing polyelectrolyte. We have used micron-scale chemical surface patterns of oligoethylene oxide, alternating with charged groups such as carboxylate acids or amines, to guide the deposition of polyelectrolyte multilayers.<sup>15–18</sup> Using this approach, it is possible to assemble

\* To whom correspondence should be addressed.

<sup>†</sup> Department of Chemical Engineering.

<sup>‡</sup> Assistant Professor, Materials Science and Engineering.

(1) Hester, J.; Banerjee, P.; Mayes, A. *Macromolecules* **1999**, *32*, 1643–1650.

(2) Golander, C.-G.; Herron, J. N.; Lim, K.; Claesson, P.; Stenius, P.; Andrade, J. D. In *Poly(Ethylene Glycol) Chemistry: Biotechnical and Biomedical Applications*; Harris, J. M., Ed.; Plenum Press: New York, 1992; pp 221–245.

(3) Lee, J. H.; Kopecek, J.; Andrade, J. D. *J. Biomed. Mater. Res.* **1989**, *23*, 351–368.

(4) Jeon, S. I.; Lee, J. H.; Andrade, J. D. *J. Colloid Interface Sci.* **1991**, *142*, 149–158.

(5) Jeon, S. I.; Andrade, J. D. *J. Colloid Interface Sci.* **1991**, *142*, 159–166.

(6) Oosterhelt, F.; Rief, M.; Gaub, H. E. *New J. Phys.* **1999**, *1*, 1–11.

(7) Grodzinsky, A.; Ortiz, C. Private communication.

(8) Mrksich, M.; Chen, C. S.; Xia, Y. N.; Dike, L. E.; Ingber, D. E.; Whitesides, G. M. *Proc. Natl. Acad. Sci. U.S.A.* **1996**, *93*, 10775–10778.

(9) Mrksich, M.; Dike, L. E.; Tien, J.; Ingber, D. E.; Whitesides, G. M. *Exp. Cell Res.* **1997**, *235*, 305–313.

(10) Mrksich, M.; Whitesides, G. M. In *Poly(Ethylene Glycol): Chemistry and Biological Applications*; Harris, J. M., Zalipsky, S., Eds.; ACS Symposium Series Vol. 680; American Chemical Society: Washington, DC, 1997; pp 361–373.

(11) Harder, P.; Grunze, M.; Dahint, R.; Whitesides, G. M.; Laibinis, P. E. *J. Phys. Chem. B* **1998**, *102*, 426–436.

(12) Wang, R. L. C.; Kreutzer, H. J.; Grunze, M. *J. Phys. Chem. B* **1997**, *101*, 9767–9773.

(13) Feldman, K.; Hahner, G.; Spencer, N. D.; Harder, P.; Grunze, G. *J. Am. Chem. Soc.* **1999**, *121*, 10134–10141.

(14) Netz, R. R. *Eur. Phys. J. E* **2000**, *3*, 131–141.

(15) Hammond, P. T.; Whitesides, G. M. *Macromolecules* **1995**, *28*, 7569–7571.

a broad array of patterned composite films onto surfaces, including conducting and luminescent polymers, electroluminescent polymers,<sup>19</sup> and low molar mass dyes, and nanometer- to micron-sized colloidal particles.<sup>20</sup> However, we have recently reported that for certain sets of synthetic polyelectrolytes, the oligoethylene oxide functional group appears to promote rather than discourage deposition over a certain pH range.<sup>19</sup> It was found that weak polyelectrolytes that are hydrophobic in nature, including poly(methacrylic acid), which has a pendant methyl group, and poly(allylamine hydrochloride) (PAH), which has a hydrophobic backbone, will preferentially adsorb to an oligoethylene oxide functionalized self-assembled monolayer (EG SAM) versus an acid-functionalized monolayer (COOH SAM). This adsorption behavior is very reproducible, and we have used the phenomenon to direct different multilayer films side-by-side on a surface, generating laterally patterned functional thin films based on the nature of the copolycation.<sup>21</sup> It is the goal of this work to further investigate the nature of this adsorption selectivity and its dependence on pH utilizing chemical force microscopy (CFM).

Control studies performed on continuous as well as patterned films confirmed that at pH 4.8, polyelectrolyte multilayers containing the hydrophobic PAH, which is cationic and partially protonated, adsorbed in larger quantities on the EG SAM rather than on the partially ionized negatively charged COOH/COO<sup>-</sup> SAM ( $pK_a$  (surface) = 5.2<sup>22</sup>) surface.<sup>19</sup> In contrast, hydrophilic linear polyethyleneimine (LPEI), which is cationic but only 50% protonated at pH = 5,<sup>23,24</sup> adsorbs consistently on the COOH/COO<sup>-</sup> region, with very little deposition on the EG surface. Figure 1 contains the structures of these two polyamines, as well as the two surface functional COOH and EG SAMs. These polyamines are an ideal choice for an examination of hydrophobic versus hydrophilic secondary interactions, electrostatic forces, and steric interactions, because they have similar chemical composition but their architectures are quite different, with an all-hydrocarbon backbone in one case and a heteroatomic, hydrophilic backbone in the other.

Although attractive interactions between PAH and the water-soluble, hydrated poly(ethylene oxide) are in some ways counterintuitive, the hydrophobic character of the ethylene oxide segment has been supported by surface force measurements and thermodynamic analysis.<sup>4,25</sup> It also appears from other studies that adventitious adsorption of proteins can occur on PEO and EG SAM surfaces under certain conditions<sup>11,12,26</sup> and with certain proteins.<sup>27,28</sup> Recent surface force apparatus experiments by Leckband and co-workers also suggest that PEO can undergo adhesive interactions with the protein streptavidin when the two material systems are forced together,

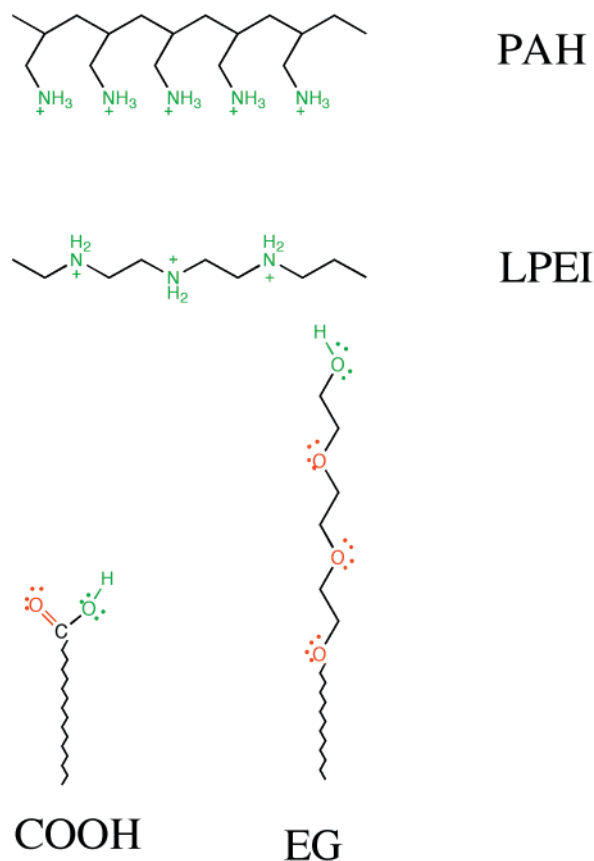


**Figure 1.** Molecular structures of PAH, LPEI, and surface functional COOH and EG SAMs.

presumably due to interactions with hydrophobic functional groups on the protein surface.<sup>27,28</sup> Ongoing studies of protein-PEO interactions confirm the complexity of interactions between these two systems.<sup>29</sup> Grunze and co-workers have found adhesive interactions between proteins and short oligoether segments of alkanethiols adsorbed on silver surfaces, for which the conformation of the oligoether segment is in the all-trans form.<sup>11</sup> The observations from protein studies confirm the possibility of hydrophobic interactions with PEO functional systems. It is important to note that proteins differ significantly from the synthetic, linear polyelectrolytes examined here, in that they exhibit unique folded, hierarchical secondary, tertiary, and quaternary structures and may undergo very specific interactions with other functional systems. On the other hand, the charged nature of the synthetic polyions, their dual hydrophobic and hydrophilic nature, and their macromolecular size are analogous to properties of proteins, allowing us to make some general comparisons between these two different macromolecular systems.

In this paper, we seek to examine directly the intermolecular interactions between the commercial synthetic polyamines PAH and LPEI with COOH- and EG-functionalized SAM surfaces using the technique of chemically specific high-resolution force microscopy. The correlation between adhesive forces and the observed selectivity of multilayers on patterned surfaces will be addressed through comparison with quantitative multilayer selec-

(16) Clark, S. L.; Montague, M.; Hammond, P. T. *Supramol. Sci.* **1997**, *4*, 141–146.

(17) Clark, S. L.; Hammond, P. T. *Adv. Mater.* **1998**, *10*, 1515–1519.

(18) Jiang, X.-P.; Hammond, P. T. *Langmuir* **2000**, *20*, 8501–8509.

(19) Clark, S. L.; Hammond, P. T. *Langmuir* **2000**, *16*, 10206–10214.

(20) Chen, K. M.; Jiang, X.-P.; Kimerling, L. C.; Hammond, P. T. *Langmuir* **2000**, *16*, 7825–7834.

(21) Jiang, X.-P.; Clark, S. L.; Hammond, P. T. *Adv. Mater.* **2001**, *13*, 1669–1673.

(22) van der Vegte, E. W.; Hadziioannou, G. *J. Phys. Chem. B* **1997**, *101*, 9563–9569.

(23) Weyts, K. F.; Goethals, E. J. *Makromol. Chem., Rapid Commun.* **1989**, *10*, 299–302.

(24) Smits, R. G.; Koper, G. J. M.; Mandel, M. *J. Phys. Chem.* **1993**, *97*, 5745–5751.

(25) Claesson, P. M.; Paulson, O. E. H.; Blomberg, E.; Burns, N. L. *Colloids Surf., A* **1997**, *123–124*, 341–353.

(26) Grunze, M. Personal communication.

(27) Sheth, S. R.; Leckband, D. E. *Proc. Natl. Acad. Sci. U.S.A.* **1997**, *94*, 8399–8404.

(28) Sheth, S. R.; Efremova, N.; Leckband, D. E. *J. Phys. Chem. B* **2000**, *104*, 7652–7662.

(29) Rixman, M.; Ortiz, C. Paper in preparation.

tivity data obtained in our earlier work.<sup>19</sup> This information will impact the ability to control the adsorption of different charged species on a given surface, presenting a means of directing two or more multilayer films to different regions of a surface based on secondary interactions. More broadly, a greater understanding of the nature of synthetic polyanion adsorption on both charged acid surfaces and surfaces containing PEO and its oligomers will ultimately provide insights into protein adsorption on such surfaces, contributing to the development and design of functional biosurfaces, and greater control of protein deposition on biomaterial surfaces.

## 2. Experimental Section

**2.1. Preparation and Characterization of Polyamine-Modified Colloidal Sphere Probes.** **2.1.1. Preparation of Polyamine-Modified Colloidal Microspheres.** Micron-size colloidal spheres were attached to the end of microfabricated cantilevers and used as force probes for the measurement of surface interactions.<sup>30,31</sup> In this study, each polyamine was covalently bound to polystyrene (PS) microspheres using a surface grafting technique in which electron beam irradiation is used to generate free radicals that lead to the formation of C–C bonds between the surface and randomly along the polymer backbone. The PAH in the chloride salt form was purchased from Aldrich, with MW 50 000–65 000. LPEI was purchased from Polysciences Inc., with MW 25 000. Polymers were used as received. The schematic of grafting polyamine on sulfated PS colloids with electron irradiation is shown in Figure 2a. This general approach has been used for a broad range of polymers.<sup>32,33</sup> To ensure attachment of a surface layer of polyamine, each positively charged polyamine was first electrostatically adsorbed to negatively charged sulfate-functionalized polystyrene latex spheres prior to irradiation. The particles used had a diameter of  $7.9 \pm 0.85 \mu\text{m}$  and were dispersed in a surfactant-free aqueous colloidal suspension at a concentration of  $4.0 \pm 0.1 \text{ g}/100 \text{ mL}$  (Interfacial Dynamics Corp., Portland, OR). The number of charged groups per particle measured by the manufacturer is  $6.9 \times 10^7$ . A 2 mL aliquot of the above latex suspension was added to 2 mL of a 20 mM aqueous polyamine solution (concentration based on repeat unit molar mass, pH adjusted to 5 for LPEI which is ~50% ionized at pH 5, no pH adjustment for PAH which is already highly ionized) and allowed to sit overnight with occasional stirring. With this ratio, amine groups are in an excess of 580 times for LPEI and 1160 times for PAH. An electron beam dosage of 6 Mrad was then applied to the latex suspensions, which still contained free polyamine in solution, to generate free radicals on the surface of the particles. The free radicals induce cross-linking of chains at and near the latex sphere surface, resulting in polyamines covalently grafted to the PS spheres. The suspensions were then filtered and rinsed copiously with deionized water.

**2.1.2. Characterization of Polyamine-Modified Colloidal Microspheres.** The presence of polyamine was confirmed by X-ray photoelectron spectroscopy (XPS, Axis Ultra, Kratos Analytic). The atomic concentration of N measured at a  $90^\circ$  takeoff angle was 4.3% for PAH-modified spheres and 5.4% for LPEI-modified spheres. The penetration depth of XPS at this angle is approximately 30–100 Å; therefore, the atomic concentrations are diluted by a thin layer of the polystyrene latex. The atomic ratio of N/S (S from sulfate groups on the latex spheres) was 29 for the PAH-modified spheres and 34 for the LPEI-modified spheres. These ratios indicate that the amine groups greatly outnumber the underlying sulfate groups on the latex sphere. The surface group density of the sulfate groups on the spheres was determined by the manufacturer using conductometric titration and determined to be relatively low. Based on the known surface

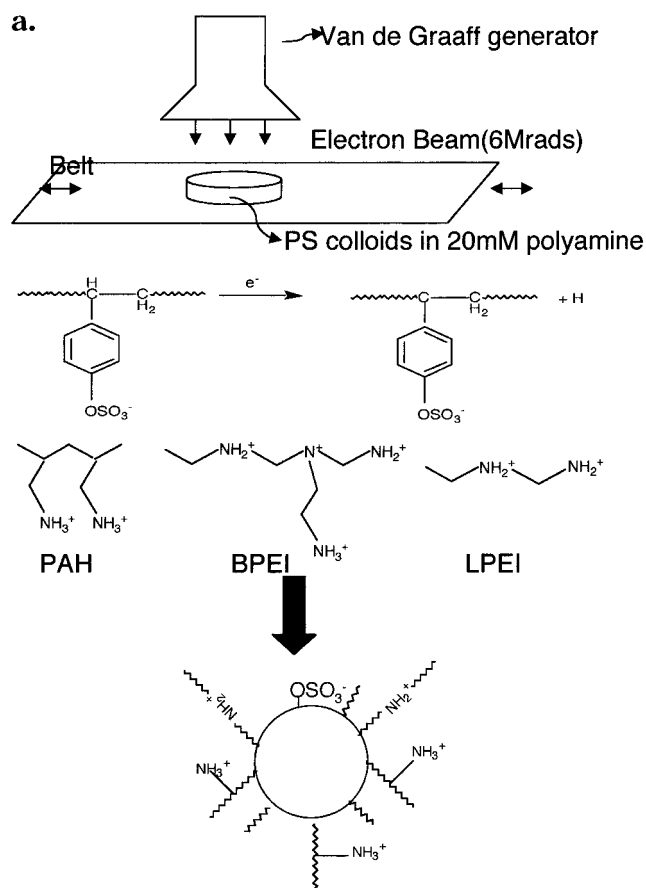


**Figure 2.** (a) The schematic of grafting polyamine on sulfated PS colloids with electron irradiation; (b) fluorescence image of LPEI-modified polystyrene latex spheres stained by fluorescent dye PSA.

concentrations of sulfate groups (provided by the manufacturer), we can calculate the number of amine groups per particle to be  $2.0 \times 10^9$  for the PAH-modified probe and  $2.34 \times 10^9$  for the LPEI-modified probe. Assuming a  $20 \text{ \AA}^2$  area per functional group, a single highly packed amino-terminated self-assembled monolayer on the colloidal sphere would yield approximately  $1 \times 10^9$  amine groups per particle. We assume the presence of a hairy layer of loosely packed polymer chains on the particle surface. The polymer-modified spheres allow greater amine densities due to the presence of dangling polymer segments. The presence of positive charge on the polyamine-modified spheres was confirmed via the attachment of negatively charged fluorescent dye 1,3,6,8-pyrenetetrasulfonic acid (PSA, from Molecular Probes). A 1 mL aliquot of  $1 \mu\text{M}$  PSA was added to 3 mL of a very dilute polyamine-modified sphere suspension ( $\sim 1 \text{ ppm}$ ) and kept at room tem-

(30) Ducker, W. A.; Senden, T. J.; Pashely, R. M. *Nature* **1991**, *353*, 239–241.

(31) Ducker, W. A.; Senden, T. J.; Pashely, R. M. *Langmuir* **1992**, *8*, 1831.

(32) Sofia, S. J.; Merrill, E. W. *J. Biomed. Mater. Res.* **1998**, *40*, 153–163.

(33) Allgor, S. J. S.; Merrill, E. W. *Mater. Res. Soc. Symp. Proc.* **1996**, *414*, 59–64.

perature for 2 h. The suspension was then centrifuged at 3000 rpm for 10 min, and the supernatant was decanted. The remaining set of spheres was diluted with deionized water and dropped on a glass slide for observation using the fluorescence microscope. The resulting image is shown in Figure 2b for LPEI-modified latex spheres. The fluorescence indicates the presence of strong positive charge due to the polyamine attached to the polystyrene colloid surface. Zeta potential analysis (Brookhaven Instruments) was also used to verify the presence of positively charged polyamine on the particle surface. In general, this approach allows the covalent grafting of polyamines on negatively charged PS spheres and thus ensures that the adsorbed polyamine will not detach even at extreme pH.

**2.1.3. Attachment and Characterization of Polyamine-Modified Colloidal Microspheres to Microfabricated Cantilevers.** The polyamine-modified microsphere was then attached to the free end of the microfabricated V-shaped tipless silicon nitride cantilever (Digital Instruments, length = 200  $\mu\text{m}$ , nominal spring constant  $k = 0.12$  N/m, actual spring constant measured by the thermal oscillation method<sup>34</sup>  $\sim 0.06$  N/m) with an epoxy resin (epoxy-patch, The Dexter Corp.) using a three-dimensional microtranslation stage (Edmund Scientific) under a stereomicroscope. Figure 3a shows a scanning electron microscope (SEM, FEI/Philips XL30 FEG ESEM) image of the LPEI-modified microsphere attached to the end of the cantilever. A different cantilever and microsphere were used for each of the polyamine experiments. Upon completion of the surface force measurements, the radius of each latex microsphere probe was measured using a SEM.

**2.2. Preparation of SAM Surfaces.** Polycrystalline gold substrates, used for thiolate COOH SAM and EG SAM attachment, were prepared by thermal evaporation at room temperature of 100  $\text{\AA}$  Cr as an adhesion promotion layer, followed by 1000  $\text{\AA}$  Au onto a silicon wafer. An atomic force microscopy (AFM) topographic image taken with D3000 tapping mode in air on 1  $\mu\text{m}^2$  region is shown in Figure 3b and was used to determine the surface roughness. Typically, the root mean square (rms) roughness of the gold substrates was 2.2 nm and the gold island size ranged from 45 to 80 nm. V-shaped, gold-coated silicon nitride cantilever/probe tips (Thermomicroscopes, Inc., unsharpened *Microlevers*, nominal tip radius  $\sim 50$  nm, length = 180  $\mu\text{m}$ , nominal spring constant  $k = 0.05$  N/m, actual spring constant measured by the thermal oscillation method  $\sim 0.04$  N/m) were used for SAM versus SAM control experiments and prepared in the same way. Gold substrates were rinsed by absolute ethanol, followed by a nitrogen blow dry just before use. COOH- and EG-functionalized SAMs were formed by immersion of gold substrates into a 2 mM absolute ethanol solution of 11-mercaptoundecanoic acid  $\text{HS}(\text{CH}_2)_{11}\text{COOH}$  (Aldrich, 95%) or a 2 mM absolute ethanol solution of oligoethylene glycol terminated alkanethiol  $\text{HS}(\text{CH}_2)_{11}(\text{OCH}_2\text{CH}_2)_3\text{OH}$  (synthesized according to ref 35) for a minimum of 12 h. For the SAM-SAM control experiments, COOH SAMs and  $\text{CH}_3$  SAMs were formed on both gold substrates and gold-coated probe tips by immersing the substrates and probe tips into a 2 mM  $\text{HS}(\text{CH}_2)_{11}\text{COOH}$ /ethanol solution or a 2 mM ethanol solution of 1-dodecanethiol  $\text{HS}(\text{CH}_2)_{11}\text{CH}_3$  (Aldrich, 98%) for a minimum of 12 h. The gold-coated probe tips, which were usually prepared in a batch of 20 and stored in an ordinary tip container, were cleaned by piranha solution for 2 min and rinsed with deionized water and ethanol, followed by a nitrogen blow dry prior to use. Figure 3c shows a SEM (JEOL 6320FV field-emission high-resolution SEM) image of the gold-coated probe tip with an end radius of approximately 63 nm. Propylaminosilane SAMs were formed on Si substrates by immersing piranha-cleaned Si substrates into a 2 mM ethanol solution of amino-propyltrimethoxy silane (Aldrich, 97%) for 2 h. All chemicals were used as received.

**2.3. High-Resolution Force Spectroscopy (HRFS) Measurement Using the Molecular Force Probe (MFP).** **2.3.1. Instrumentation.** HRFS experiments were conducted using a new cantilever-based, piconewton-sensitive instrument, the Molecular Force Probe (Asylum Research, Santa Barbara, CA,

shown in Figure 4a) to measure force,  $F$  (nN), versus tip-sample separation distance,  $D$  (nm). Modeled on AFM technology, the MFP employs a micromachined soft, flexible cantilever with a sharp tip as a force transducer that deflects in response to the small forces between the probe tip and a sample surface. A near-IR laser beam is focused on the backside of the end of the cantilever and directed with a mirror into a split position-sensitive photodiode (PSPD). The MFP has an open fluid cell design with an optical (video) microscope located in the base, making it ideal to work on polymeric and biological samples. An adjustable laser focus, novel optic lever geometry, and a low coherence light source optimize response and minimize interference reflections from reflective samples. A piezoelectric translator (10  $\mu\text{m}$  range) located on a flexure plate in the head incrementally moves the tip toward the sample in the  $z$ -direction perpendicular to the sample plane ("approach") and away from the sample ("retract") at a constant rate. A LVDT (linearly variable differential transformer) position sensor ( $<3$   $\text{\AA}$  noise in 0.1–1 kHz bandwidth, 15  $\mu\text{m}$  travel, 0.02% linearity), also located on the flexure plate in the head, quantifies the distance that the  $z$ -piezo moves the cantilever directly, thus eliminating error due to piezo hysteresis and other nonlinearities and also reducing or eliminating the effects of thermal drift over long time scales. The probe tip in this instrument is electrically grounded.

**2.3.2. Conversion of Raw Data and Measurement Errors.** Igor Pro (Wavemetrics) software routines were used for conversion of the raw data, that is, photodiode sensor output (V) versus LVDT output (nm) into force,  $F$  (nN), versus tip-sample separation distance,  $D$  (nm). The vertical sensor output difference of the top minus bottom quadrants of the PSPD normalized by the sum total PSPD output,  $s$  (V) =  $(T - B)/(T + B)$ , is converted into cantilever deflection,  $\delta$  (nm), by assuming that the change in the  $z$ -piezo movement (equal to the change in movement of the base of the probe tip),  $dz$ , measured by the LVDT output (nm) is equivalent to the change in cantilever deflection,  $d\delta$  (nm), in the repulsive, contact regime of "constant compliance":

$$\delta \text{ (nm)} = s \text{ (V)} \times \text{IOLS (nm/V)} \quad (1)$$

where the IOLS is the "inverse optical lever sensitivity" (nm/V) and is equal to the inverse slope of the sensor versus LVDT output curve in the constant compliance regime. The force is then calculated by using Hooke's law for a linear elastic spring:

$$F \text{ (nN)} = k_c \text{ (N/m)} \times \delta \text{ (nm)} \quad (2)$$

where  $F$  (nN) is the interaction force and  $k_c$  is the cantilever spring constant (N/m).  $k_c$  was determined for each individual cantilever according to a nondestructive thermal oscillation method described in the literature.<sup>34</sup> The usual convention of positive (+) for repulsive forces and negative (–) for attractive forces was employed. The zero force baseline was taken from data obtained when the cantilever was undeflected far away from the surface ( $\sim 1000$  nm). The error in force measurements is due to calculation of the IOLS ( $\pm 5\%$ ), the spring constant calibration ( $\pm 20\%$ ), and nonlinearities of the photodetector associated with the finite size of the laser spot ( $\pm 2\%$ ).

The LVDT signal output (V) was converted into  $z$ -piezo distance,  $z$  (nm), by calibration at Asylum Research, Inc. via interferometry. The LVDT was found to have a sensitivity of 1.47  $\mu\text{m/V}$ .  $z$  (nm), and was converted into the tip-sample separation distance,  $D$  (nm), by correcting for the cantilever displacement due to the applied force:

$$D \text{ (nm)} = z \text{ (nm)} - \delta \text{ (nm)} \quad (3)$$

where  $\delta$  is calculated from eq 2. The vertical region of apparent infinite slope in the high-force, constant compliance regime was set to  $D = 0$ . For high-density polymer brushes, it has been shown that there is an inherent error in this assumption due to the presence of a compacted, incompressible polymer layer which is approximately equal to the thickness of the polymer layer in the dry state for lower molecular weights ( $\text{MW} < 25\,000$ ).<sup>36,37</sup> Hence,

(34) Hutter, J. L.; Bechhoefer, J. *Rev. Sci. Instrum.* **1993**, *64*, 1868.  
 (35) Pale-Grosdemange, C.; Simon, E. S.; Prime, K. L.; Whitesides, G. M. *J. Am. Chem. Soc.* **1991**, *113*, 583.

(36) Yamamoto, S.; Ejaz, M.; Tsujii, Y.; Fukuda, T. *Macromolecules* **2000**, *33*, 5608–5612.

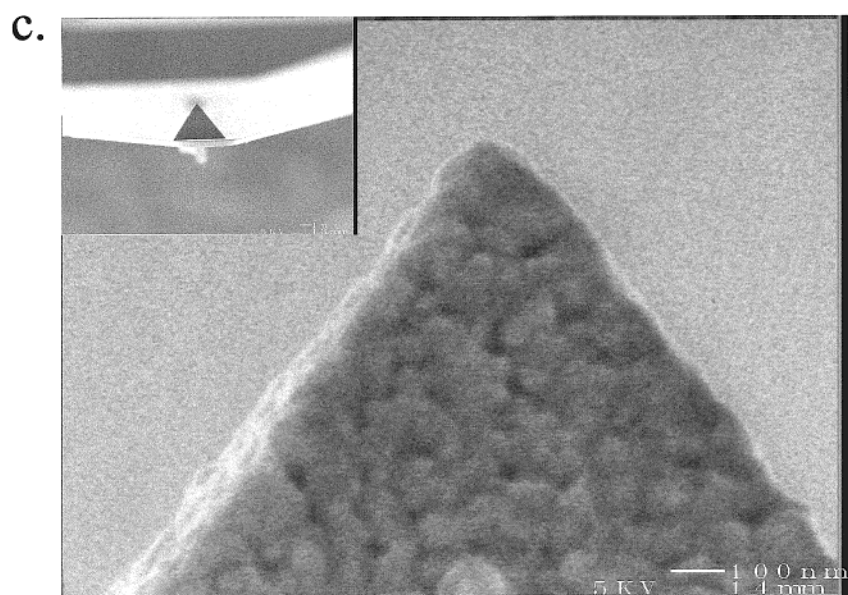
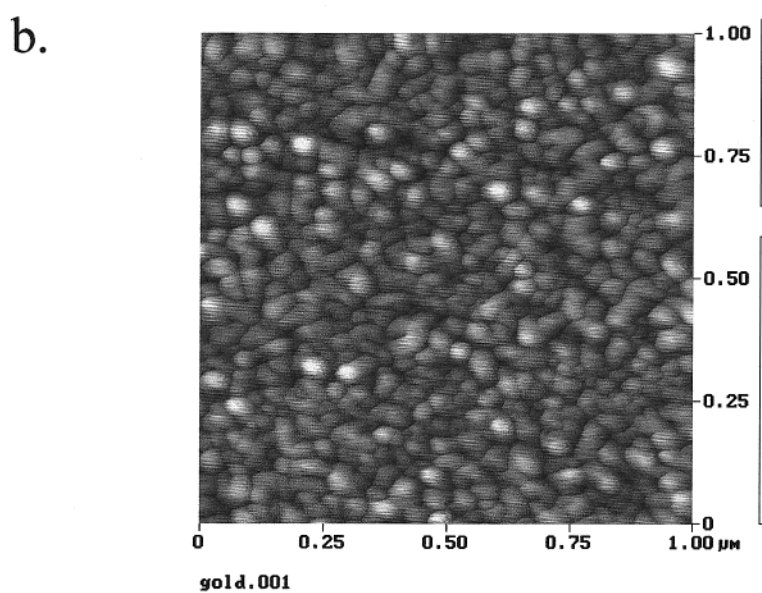
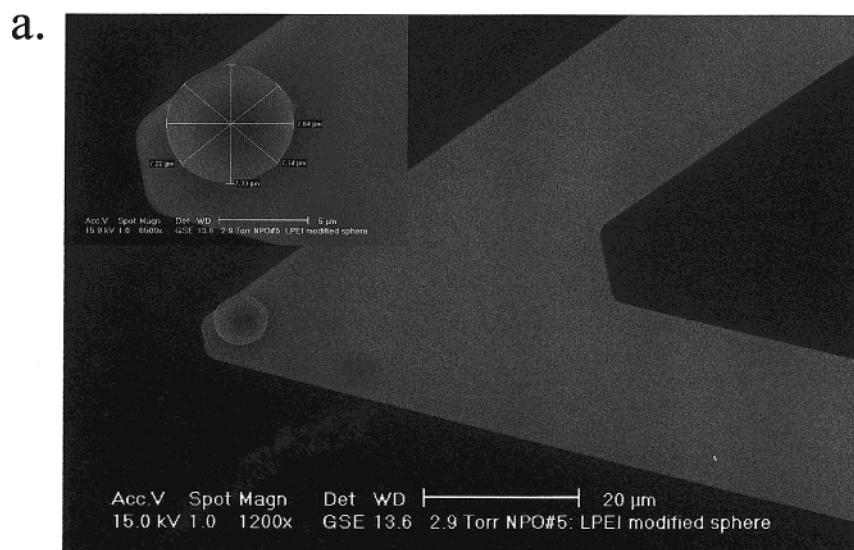


**Figure 3.** (a) A SEM image of the LPEI-modified microsphere on the end of the V-shaped cantilever; (b) an AFM topographic image of the gold substrate; (c) a SEM image of the gold-coated tip used in control experiments.

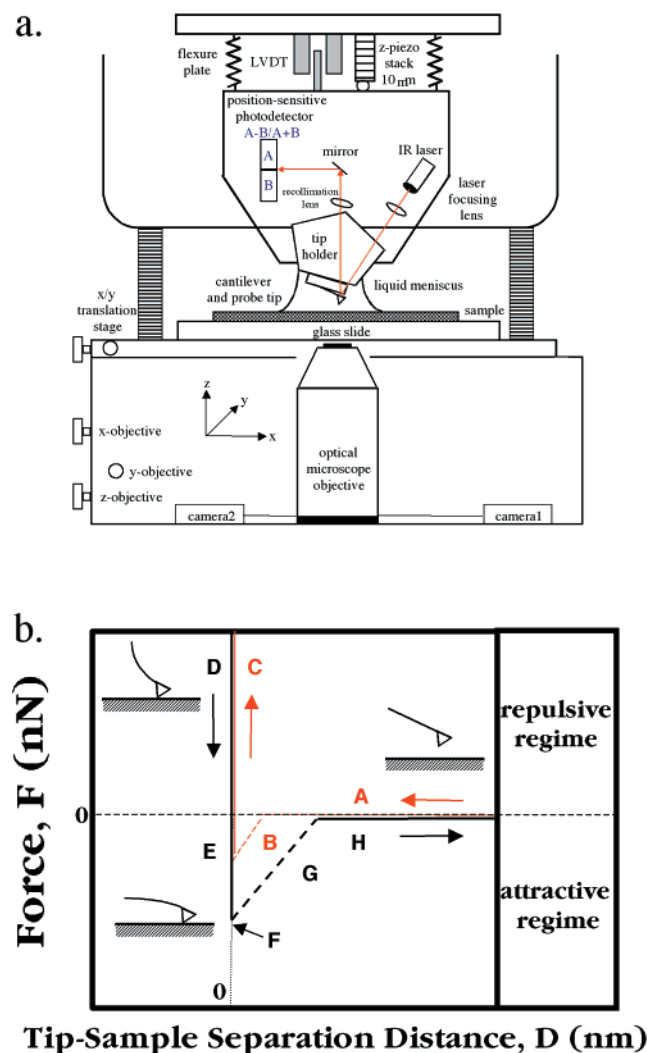


**Figure 4.** (a) Schematic of the MFP measurement setup. (b) Typical force,  $F$ , versus tip-surface separation distance,  $D$ , on a hard substrate ( $k \ll k_{\text{sample}}$ ): (approach) A, no interaction with surface; B, cantilever instability and jump-to-contact; C and (retract) D, constant compliance contact regime; E, surface adhesion; F, adhesion force; G, pull-off from surface; H, no interaction with surface.

the tip-surface separation distance will be offset along the  $x$ -axis by this unknown thickness value. Although the absolute tip-surface separation distance has this inherent error, much qualitative information can be gained from the shape and slope of the force curve and in addition, our primary focus and discussion will be the magnitude of the jump-to-contact and pull-off adhesion forces which can be measured quantitatively.

**2.3.3. Typical Force versus Distance Curve.** Figure 4b shows a typical force curve on a stiff substrate using a relatively soft cantilever ( $k_c \ll k_{\text{sample}}$ ) (e.g., for a SAM probe tip versus SAM surface). Far from the surface, the cantilever remained undeflected and the net force is zero (Figure 4b, region A). As the probe approaches close to the surface, typically nonspecific, attractive tip-surface interactions are present (e.g., due to van der Waals forces, etc.) and the cantilever exhibits a mechanical instability which results in a discontinuous “jump-to-contact” (Figure 4b, region B). This is due to the fact that the gradient of the interaction force exceeds the cantilever spring constant. All data in this region of the force curve are lost, and the slope of this line is just equal to the cantilever spring constant,  $dF/dD = k_c$ . After surface contact is made, a region with an apparent infinite slope (which is set to  $D = 0$ ) is observed (Figure 4b,

region C) which is due to the fact that the spring constant of the cantilever is much less than the stiffness of the substrate. Hence, little or no deformation of the sample takes place and the cantilever and sample move together in unison. When a force of a few nanonewtons is achieved, the piezo then reverses direction and the tip is moved away from the sample (retract) (Figure 4b, region D). Surface adhesion is usually present (Figure 4b, region E), and once again the cantilever exhibits a mechanical instability which leads to a sudden “pull-off” point which is defined as the surface adhesion force (Figure 4b, region F).

**2.3.4. HRFS Experimental Parameters and Data Analysis.** The total force versus separation distance between the polyamine-modified colloidal sphere probe and SAM (i.e., COOH and EG) surfaces was measured in a 10 mM buffer solution ranging from pH 2 to pH 7 at room temperature using the MFP ( $z$ -piezo velocity  $v = 0.5 - 1.0 \mu\text{m/s}$ , piezo range =  $0.5 - 1 \mu\text{m}$ , rate of data acquisition = 2000 points/s). The buffer solutions were made according to the CRC Handbook of Chemistry and Physics (78th edition, 1997–1998) but diluted with deionized (DI) water to a final ionic strength equal to 10 mM. All water was deionized with the Milli-Q Plus ultrapure water system (Millipore, Bedford, MA) to 18 M $\Omega$  cm resistivity. Accurate pH values were then measured with a Beckman  $\Phi 10$  pH meter after dilution. Potassium hydrogen phthalate (Aldrich, 99.99%) was used for the preparation of buffer solutions in the range of pH 2–5.8. Potassium dihydrogen phosphate (Aldrich, 99%) was used for the preparation of buffer solutions in the range of pH 5.8–8.0. For each pair of polyamine-modified probe and SAM surface, over 100 force curves were collected on at least 5 different spots on each SAM surface. Representative force versus distance curves for individual experiments are reported rather than averaged curves, so that the fine details of the interaction are not averaged out. Statistical analysis was done on the jump-to-contact and adhesion forces with means and standard deviations reported.

### 3. Results and Discussion

**3.1. Control Experiments: Interaction between SAM Probe Tips and SAM Surfaces as a Function of pH.** Chemical force microscopy (CFM) is the technique whereby chemical specificity is added to AFM by deliberate derivatization of an AFM probe.<sup>38</sup> Typically, a variety of functional groups are obtained by modifying a gold-coated AFM cantilever with alkanethiol SAMs with the desired terminal group. The electrostatic, hydrogen bonding, and hydrophobic interactions between surfaces terminated with various functionalities have been studied in a range of solvents using this approach, including investigations of COOH–COOH, NH<sub>2</sub>–NH<sub>2</sub>, COOH–NH<sub>2</sub>, and CH<sub>3</sub>–CH<sub>3</sub> tip-surface functional group pairs.<sup>39–44</sup> Literature data of the adhesion forces between functional groups in aqueous media are summarized in Table 1. The absolute magnitude of the adhesion force will vary depending on the details of the experimental conditions (e.g., sample preparation and cleanliness, surface and tip roughness, tip radius, etc.). A series of control experiments were first carried out with the MFP using various alkanethiol SAM derivatized probe tips versus SAM surfaces in aqueous solution (ionic strength IS = 0.01 M). All of the force curves appeared similar in form to that shown schematically in

(38) Frisbie, C. D.; Noy, A.; Rozsnyai, L. F.; Wrighton, M. S.; Lieber, C. M. *Science* **1994**, *265*, 2071–2074.

(39) Sinniah, S. K.; Steel, A. B.; Miller, C. J.; Reutt-Robey, J. E. *J. Am. Chem. Soc.* **1996**, *118*, 8925–8931.

(40) van der Vegte, E. W.; Hadziioannou, G. *Langmuir* **1997**, *13*, 4357–4368.

(41) Ito, T.; Namba, M.; Buhlmann, P.; Umezawa, Y. *Langmuir* **1997**, *13*, 4323–4332.

(42) Vezenov, D. V.; Noy, A.; Rozsnyai, L. F.; Lieber, C. M. *J. Am. Chem. Soc.* **1997**, *119*, 2006–2015.

(43) Wenzler, L. A.; Moyes, G. L.; Raikar, G. N.; Hansen, R. L.; Harris, J. M.; Beebe, T. P., Jr.; Wood, L. L.; Saavedra, S. S. *Langmuir* **1997**, *13*, 3761–3768.

(44) Noy, A.; Frisbie, C. D.; Rozsnyai, L. F.; Wrighton, M. S.; Lieber, C. M. *J. Am. Chem. Soc.* **1995**, *117*, 7943–7951.

(37) Yamamoto, S.; Ejaz, M.; Tsujii, Y.; Matsumoto, M.; Fukuda, T. *Macromolecules* **2000**, *33*, 5602–5607.

Table 1. Adhesion Forces between Functional Groups from Literature Data

functional group pair (tip-surface)	monolayer chain length	medium	adhesion force $F$ (nN)	ref	tip radius $R$ (nm)	normalized adhesion force ( $F/R$ , mN/m)
COOH-COOH	thiol, C <sub>11</sub>	H <sub>2</sub> O, pH < 5 <sup>a</sup>	7.0 ± 0.5	42	60	116
COOH-COOH	thiol, C <sub>11</sub>	H <sub>2</sub> O, pH < 5 <sup>a</sup>	8.5 ± 0.5	22	75	113
COOH-COOH	thiol, C <sub>11</sub>	H <sub>2</sub> O, DI	2.3 ± 1.1	39	30	77
CH <sub>3</sub> -CH <sub>3</sub>	thiol, C <sub>12</sub>	H <sub>2</sub> O <sup>a</sup>	20 ± 2.5	22	75	267
CH <sub>3</sub> -CH <sub>3</sub>	thiol, C <sub>12</sub>	H <sub>2</sub> O, DI	12.5 ± 4.4	39	30	417
NH <sub>2</sub> -NH <sub>2</sub>	silane, C <sub>3</sub>	H <sub>2</sub> O, pH > 6 <sup>a</sup>	28	42	60	467
NH <sub>2</sub> -NH <sub>2</sub>	thiol, C <sub>2</sub>	H <sub>2</sub> O, pH > 10 <sup>a</sup>	14 ± 1	22	75	187
COO <sup>-</sup> -NH <sub>3</sub> <sup>+</sup>	thiol, C <sub>11</sub> for COOH; silane, C <sub>3</sub> for NH <sub>2</sub>	DI H <sub>2</sub> O, pH 6.5	14	44	150	93
COO <sup>-</sup> -NH <sub>3</sub> <sup>+</sup>	thiol, C <sub>11</sub> for COOH; silane, C <sub>3</sub> for NH <sub>2</sub>	0.3 M NaCl in H <sub>2</sub> O pH 6.5	4.5	44	150	30

<sup>a</sup> Ionic strength IS = 0.01 M.

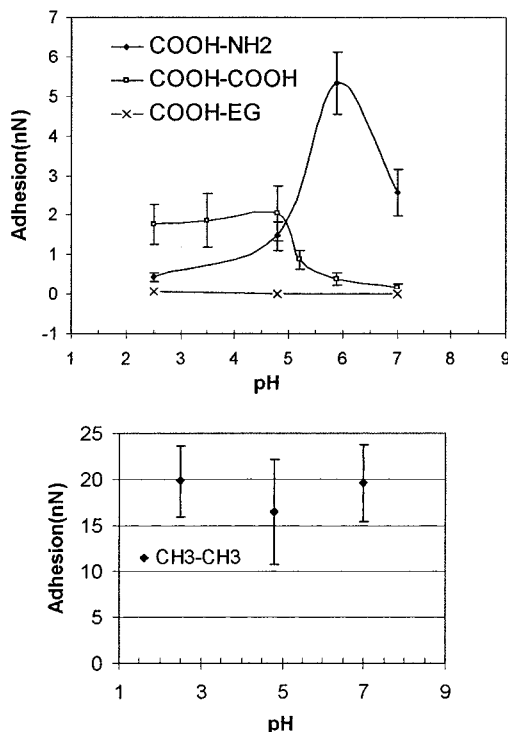


**Figure 5.** (a) Control experiments of adhesion between COOH-COOH, COOH-NH<sub>2</sub>, and COOH-EG SAM surfaces; (b) control experiments of adhesion between CH<sub>3</sub>-CH<sub>3</sub> SAM surfaces.

Figure 4b (i.e., the jump-to-contact and pull-off occur at zero separation). The results are summarized in Figure 5.

**3.1.1. COOH SAM Probe Tip versus COOH SAM Surface.** A typical titration curve was obtained for the COOH-COOH tip-surface pair which appears similar to that reported by Vezenov<sup>42</sup> and van der Vegte.<sup>22</sup> At low pH, the adhesion force is relatively strong at approximately 2 nN and is dominated by hydrogen bond dimerization between acid groups on the surface and the functionalized tip. This force corresponds to a reduced force of 32 mN/m; this value is smaller than the reported literature values, although the gold substrates and gold-coated tips are similar in preparation and size (60 nm tip). This deviation is most likely due to differences in surface roughness, which lead to lowered contact area of the tip and surface. The gold surfaces of the probe tips and gold substrates used in these experiments have a rms roughness of 2.2 nm (determined from ten 1  $\mu\text{m}^2$  size AFM images), larger than the reported 1.2 nm used in the cited studies,<sup>45,46</sup> and a grain size of ca. 70 nm as shown in Figure 3b,c. Consistent with literature reports, the adhesion force drops

dramatically when the pH approaches the pK<sub>a</sub> of the surface acid groups (~5.2). Beyond this point, the electrostatic repulsion of the COO<sup>-</sup> groups in the partially ionized SAM results in little or no adhesion and ultimate repulsion between the surfaces.

**3.1.2. COOH SAM Probe Tip versus NH<sub>2</sub> SAM Surface.** For the COOH-NH<sub>2</sub> pair, the maximum adhesion force of 5.3 nN in 10 mM buffer solution corresponds to a reduced force of 84 mN/m, close to the literature reported value of 93 mN/m (see Table 1).<sup>44</sup> The maximum value of adhesion occurs at pH 6.0, a value which falls between the surface pK<sub>a</sub> of the COOH group of 5.2 and the surface pK<sub>a</sub> for the NH<sub>2</sub> group of 7.<sup>22</sup> Electrostatic interactions are optimized at this pH range, because a large fraction of both the acid and amino groups are ionized (~70%). The relatively low adhesion force at low pH can be attributed to a combination of hydrogen bonding and a small electrostatic contribution from the weakly ionized COOH and NH<sub>3</sub><sup>+</sup> groups. At pH 7, the adhesion force also decreases from the maximum, as the degree of ionization of the amino groups begins to decrease slightly at this point.

**3.1.3. COOH SAM Probe Tip versus EG SAM Surface.** Since the ethylene glycol segment contains hydrogen bond acceptor groups in the form of the lone pair electrons on the oxygen atoms, hydrogen bonding may also occur on EG surfaces. Because the COOH group is acidic and can serve as a very strong hydrogen bond donor, surface force measurement was also done on a COOH-EG pair at different pH values (as shown in Figure 5a). The results show that only a very weak adhesion force of 0.08 nN exists at pH 2.5, and pure repulsion was observed at moderate and high pH levels. This repulsion was similar in range and magnitude to that reported in ref 13 and is attributed to hydration and electrostatic interactions.

**3.1.4. CH<sub>3</sub> SAM Probe Tip versus CH<sub>3</sub> SAM Surface.** The role of hydrophobicity has been investigated both experimentally and theoretically on a broad range of systems, including the adsorption of ionic surfactants on charged surfaces,<sup>47,48</sup> interactions between two PEO surfaces<sup>49</sup> and recently between protein and PEO,<sup>27,28,50</sup> and so forth. It is generally found from these and other

(45) McKendry, R.; Theoclitou, M.-E.; Abell, C.; Rayment, T. *Langmuir* **1998**, *14*, 2846-2849.

(46) McKendry, R.; Theoclitou, M.-E.; Abell, C.; Rayment, T. *Jpn. J. Appl. Phys., Part 1* **1999**, *38*, 3901-3907.

(47) Pashley, R. M.; McGuigan, P. M.; Ninham, B. W.; Evans, D. F. *Science* **1985**, *229*, 1088-1089.

(48) Tsao, Y.-H.; Evans, D. F.; Wennerstrom, H. *Science* **1993**, *262*, 547-550.

(49) Claesson, P. M.; Kjellander, R.; Stenius, P.; Christenson, H. K. *J. Chem. Soc., Faraday Trans. 1* **1986**, *82*, 2735-2746.

(50) Jeon, S. I.; Andrade, J. D. *J. Colloid Interface Sci.* **1991**, *142*, 159-166.

studies that hydrophobic interactions can be long ranged ( $\sim 10$ – $100$  nm), with a strength and range that greatly depend on the hydrophobicity of the surface.<sup>47</sup> In this control experiment, hydrophobic interactions were measured using a  $\text{CH}_3$ – $\text{CH}_3$  SAM tip–surface pair formed from dodecyl thiolates. The results shown in Figure 5b indicate that hydrophobic interactions are very strong in aqueous media and are pH insensitive; similar large force values in water have been measured by others.<sup>22</sup> The adhesion force in this case was found to be as high as 20 nN, or 317 mN/m; however, such strong hydrophobic interactions are the result of a highly ordered and close-packed  $\text{CH}_3$  SAM system, with a purely hydrocarbon composition. Hydrophobic effects would be weakened dramatically in systems with a smaller fraction of hydrocarbon or with less uniform or disordered hydrophobic moieties.<sup>48,51</sup> Usually, for hydrocarbon systems the observed hydrophobic interaction is 10–100 times stronger than van der Waals interactions.

The control experiments described above provide a quantitative comparison of the adhesion forces found between oppositely charged species ( $\text{COOH}$ – $\text{NH}_2$ ), hydrogen bond pairs ( $\text{COOH}$ – $\text{COOH}$  and  $\text{COOH}$ – $\text{EG}$ ), and hydrophobic species ( $\text{CH}_3$ – $\text{CH}_3$ ) as well as a confirmation of the general CFM technique utilizing the MFP instrument. These numbers give us a relative sense of the size and range of such secondary interactions in aqueous solution. Although the tip size and functionality differ for the polyamine studies, in which grafted colloidal spheres were used as probes, this control data can be used to make qualitative comparisons in the polyamine studies of the relative roles of these secondary interactions in the adhesion of the polymers to  $\text{COOH}$  and  $\text{EG}$  SAMs.

**3.2. Interactions between the LPEI Colloidal Probe and SAM Surfaces as a Function of pH. 3.2.1. LPEI Colloidal Probe versus  $\text{COOH}$  SAM Surface.** Representative force versus distance curves for pH 2.5, 4.8, and 7.0 are given in Figure 6a–c. Force curves were found to be consistent in magnitude and characteristic shape when collected at different points on the surface, indicating uniformity of the surface. In contrast to the typical force versus distance curve observed for the alkanethiol SAM–SAM control systems (Figure 4b), all of the force curves here exhibit nonlinear, long-range ( $D < 75$  nm) repulsive forces on approach. A jump-to-contact, which is thought to be the point where the outermost chain segments of the grafted polymer layer first make physical contact with the surface SAM, can only be observed at pH 2.5 and pH 4.8, implying that at these distances, attraction dominates the movement of the tip on approach at those pH levels. At these pH conditions, no detectable force is observed prior to the jump-to-contact and a jagged, nonlinear repulsive curve is seen with decreasing separation distance after the jump-to-contact, suggesting a nonuniform compression of the polymer layer. Averaged values for the jump-to-contact forces (including the normalized or reduced force/radius) taken from individual force curves are given in Table 2. On retraction, it was observed that there is always a measurable adhesive force between the LPEI probe and the  $\text{COOH}$  SAM surface at all pH values investigated. The pull-off retraction peaks take place at nonzero distances and are nonlinear and jagged in many cases, due to the gradual detachment of the probe from the surface and the accompanied polymer chain bridging and extension. Averaged values of the adhesion force (including the normalized or reduced force/

**Table 2. Jump-to-Contact and Pull-Off Forces for the LPEI Probe ( $R = 3.6 \mu\text{m}$ )<sup>a</sup>**

pH	surface	jump-to-contact force $F$ (nN)	reduced jump-to-contact force $F/R$ (mN/m)	pull-off force $F$ (nN)	reduced pull-off force $F/R$ (mN/m)
2.5	COOH	$1.5 \pm 0.6$	$0.42 \pm 0.16$	$8.2 \pm 0.5$	$2.28 \pm 0.14$
4.8	COOH	$1.5 \pm 0.6$	$0.42 \pm 0.16$	$13.4 \pm 2.8$	$3.72 \pm 0.78$
7.0	COOH	0	0	$2.5 \pm 0.5$	$0.69 \pm 0.14$
2.5	EG	0	0	$2.1 \pm 1.5$	$0.58 \pm 0.42$
4.8	EG	0	0	0	0
7.0	EG	0	0	0	0

<sup>a</sup> The number after  $\pm$  is a standard deviation.

radius) taken from individual force curves for the LPEI-modified colloidal sphere probe on the  $\text{COOH}$  surface are shown in Table 2. Compared to the SAM–SAM control experiments, the reduced force data for the polymer-functionalized colloidal probes are 1 or 2 orders of magnitude lower. This phenomenon may be in part due to increased surface roughness on the e-beam irradiated, grafted colloidal particles, additional steric repulsion due to the presence of polymer segments, and differences in the packing density of functional groups on the more diffuse polymer layer versus the SAM. In this study, the focus is directed toward qualitative comparisons of the adhesive interactions between the two different polyamines. Quantitative comparisons can be made within a specific polyamine type on different surfaces and at different pH conditions.

The total interaction force between the LPEI-modified probe tip and the  $\text{COOH}$  SAM functionalized surface has a number of possible attractive and repulsive components: (1) an *attractive van der Waals* force that for such a large probe radius of  $8 \mu\text{m}$  can be extremely long range, that is, beginning at  $D < 100$  nm; (2) *attractive hydrogen and ionic bonding* between the amine groups on the LPEI polymer chain and the  $\text{COOH}$  SAM surface which begins when the probe tip comes into physical contact with the top of the polymer layer and increases in magnitude with decreasing separation; (3) a repulsive *steric* or “overlap” force due to deformation of the polymer layer or brush in compression, which for flexible polymer chains has contributions from configurational entropy, excluded volume, and an osmotic pressure due to a local increase in chain segment concentration at the interface<sup>52</sup> (steric repulsion is directly determined by the conformation of the polymer chains at the surface and the intermolecular interactions between the polymer and the underlying substrate, begins at the top of the polymer layer, and is known to be exponentially nonlinear<sup>53,54</sup>); (4) a repulsive *electrostatic double-layer* force due to an induced surface charge at the interface between the electrolyte and insulating region in the presence of another charged surface;<sup>7</sup> and (5) a repulsive *hydration* force due to the displacement of hydrated, adsorbed surface counterions and due to the energy needed to dehydrate the bound counterions, which presumably retain some of their water of hydration on binding. This force has been observed experimentally on different hydrophilic charged surfaces in electrolyte solutions of intermediate and high ionic strength and known to be very short range ( $< 4$  nm), monotonic, and exponentially repulsive.<sup>55</sup>

(52) de Gennes, P.-G. *Adv. Colloid Interface Sci.* **1987**, *27*, 189–209.

(53) Biggs, S. *Langmuir* **1995**, *11*, 156–162.

(54) O’Shea, S. J.; Welland, M. E.; Rayment, T. *Appl. Phys. Lett.* **1992**, *61*, 2240–2242.

(55) Israelachvili, J. N. *Intermolecular and Surface Forces*, 2nd ed.; Academic Press: London, 1991; Section 13.5 and references therein.

(51) Claesson, P. M.; Christenson, H. K. *J. Phys. Chem.* **1988**, *92*, 1650–1655.

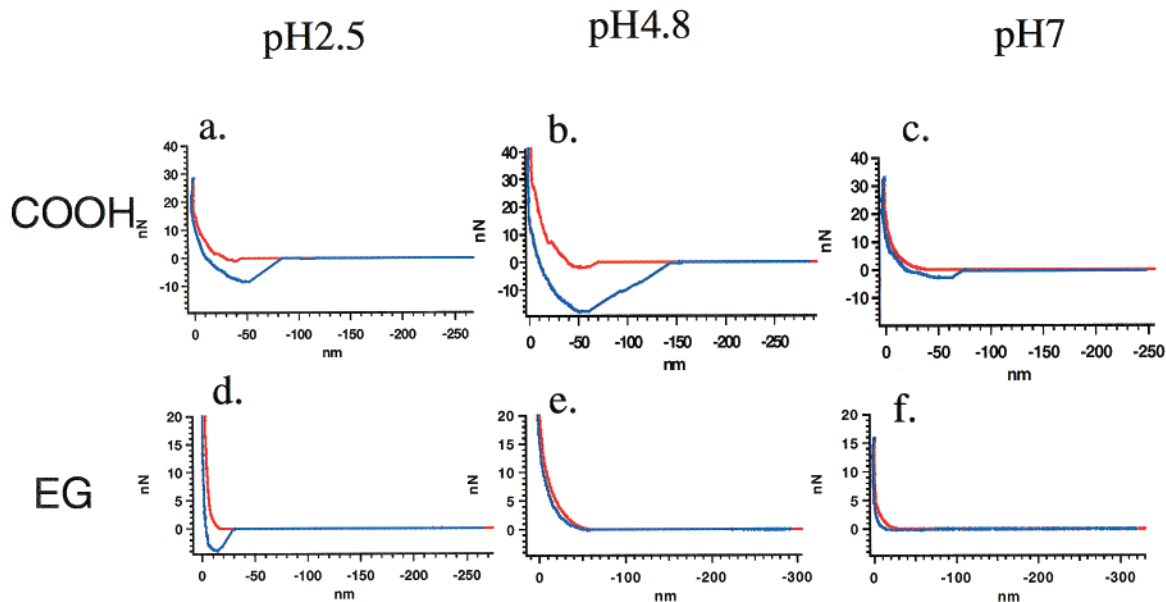


**Figure 6.** Representative in situ force–distance curves of the LPEI colloid probe on the COOH SAM and EG SAM surfaces: (a) on COOH SAM at pH 2.5; (b) on COOH SAM at pH 4.8; (c) on COOH SAM at pH 7.0; (d) on EG SAM at pH 2.5; (e) on EG SAM at pH 4.8; (f) on EG SAM at pH 7.0. (Curves shown are representative samples taken from an ensemble of hundreds of measurements.)

The dramatic differences in adhesion forces for LPEI on COOH originate from changes in the attractive hydrogen and ionic bonding components of the force resulting from variation of the pH. At low pH, we are well below the  $pK_a$  of 5.2 for the COOH groups as determined by the control experiments. Given that only a small fraction of the COOH groups should be ionized at this pH, ionic bonding should contribute just a small fraction to the total adhesion, and hydrogen bonding between acid and protonated secondary amine groups is presumed to be prevalent. The magnitude of the pull-off force suggests favorable adhesive interactions between LPEI and the COOH surface at pH 2.5. As the pH is increased to 4.8, the pull-off force increases to 13.4 nN as the  $pK_a$  of the acid groups is approached, and roughly 40–50% of the acid groups become ionized. At pH 4.8, LPEI remains close to 50% ionized; its  $pK_a$  is also close to 5.0.<sup>56</sup> For this reason, ionic bonding becomes a more dominant factor in adhesion, and the attractive interactions are increased. Finally, at pH 7, the jump-to-contact force decreases to 0.0, and the pull-off force drops to 2.5 nN. In this case, we have exceeded the  $pK_a$  of LPEI, which now carries significantly less charge (approximately 30% based on literature values<sup>56</sup>). The deprotonated secondary amines in the polymer backbone undergo fairly weak attraction with the highly charged  $COO^-$  surface at this pH. Ionic interactions are fairly weak due to the low degree of ionization of LPEI, and hydrogen bonding is also significantly less important with the  $COO^-$  groups. In addition, it is generally known that the conformation of all polyamines will assume a more collapsed form as pH is increased, thus reducing the steric component of the total force.

**3.2.2. LPEI Colloidal Probe versus EG SAM Surfaces.** Representative force versus distance curves for the LPEI probe versus EG SAM at pH 2.5, 4.8, and 7.0 are given in Figure 6d–f. Typically, a smooth, nonlinear, purely repulsive approach curve is observed at all pH levels tested, with no jump-to-contact behavior. There are two possible additional repulsive interactions unique to the EG SAM layer compared to the COOH SAM: (1) an

*enthalpic* penalty for disruption of the helical backbone that PEO forms upon H-bonding with water<sup>6</sup> and (2) a hydration force due to the fact that the oligoethylene oxide layer acts as a template for the formation of an ordered water layer at the surface.<sup>12</sup> Compared to the COOH SAM, the magnitude and range of the approaching repulsive forces are much reduced. This is unexpected considering the additional repulsive forces mentioned above and indicates that the steric component is a strong function of noncovalent tip–surface interactions. Importantly, the adhesive interactions between the LPEI probe and the EG SAM are also much reduced to 2.1 nN at pH 2.5 and nonexistent (purely repulsive) at pH 4.8 and pH 7. One contribution to the adhesion force at pH 2.5 is presumably due to hydrogen bonding between the  $-NH^+$  secondary amine donors and the lone pair oxygen acceptors of the EG SAM. At pH 4.8, the number of charged groups on the LPEI backbone has begun to decrease, and under these conditions it appears that LPEI acts as a hydrated chain that is free of strong attractive hydrogen bonding interactions with EG. When the hydrated polyamine chain is pushed against the hydrated EG brush, repulsion is exhibited. It is under these conditions that EG acts as a near-perfect resist for the deposition of LPEI-based multilayers. Finally, at pH 7, when the polyamine chain is less protonated, the forces measured again indicate pull-off forces of zero and little or no adhesion.

**3.2.3. Correlation of Adhesion Forces of the LPEI Colloidal Probe with Selectivity Data.** Figure 7 shows a summary of the pull-off forces observed in LPEI/SAM systems as a function of pH. One can compare the magnitude of the forces qualitatively with the inherent driving force for adsorption and adhesion on the SAM surfaces. Polyelectrolyte multilayer systems based on LPEI are greatly influenced by the preferred region of deposition of the polyamine, as reported earlier.<sup>19</sup> The selectivity data for multilayer deposition is therefore compared directly to the surface forces on each surface. These data were taken from thickness values of multilayer polymer thin films formed from coadsorption of LPEI with PAA.<sup>19</sup> Selectivity in this case is defined as  $\{(\text{film thickness on COOH SAM} - \text{film thickness on EG SAM}) / \text{the greater}$

(56) Smits, R. G.; Koper, G. J. M.; Mandel, M. *J. Phys. Chem.* **1993**, *97*, 5745.

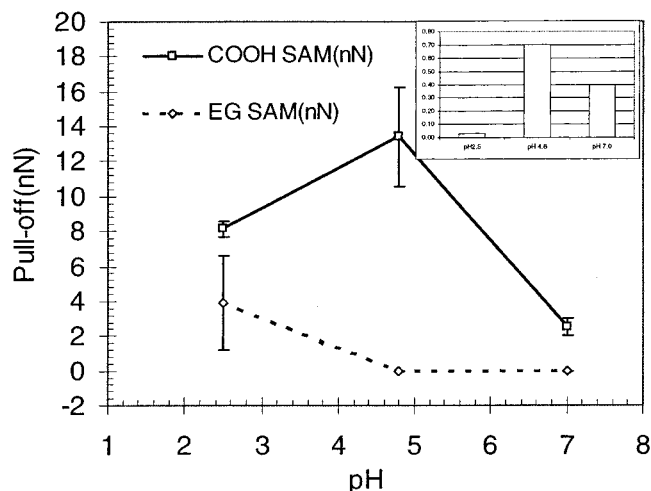


**Figure 7.** The summary of the pull-off forces observed in the LPEI probe on COOH and EG SAM systems as a function of pH. The inset shows the selectivity data from thickness measurement on multilayer films, which is defined as (film thickness on COOH SAM – film thickness on EG SAM)/the greater film thickness.

film thickness}. At low pH, the amount of LPEI/PAA multilayer adsorbed on the COOH and EG surfaces was almost equal, with significant deposition occurring on both regions. The net selectivity was a small positive value, as shown in the inset of Figure 7. This is consistent with the fact that LPEI appears to undergo strong adhesive interactions with both COOH and EG at pH 2.5. The use of PAA as a copolyanion may have further biased deposition toward the COOH surface due to acid–acid hydrogen bonding across layers. At pH 4.8, however, the EG surface becomes an excellent resist to deposition of LPEI, due to reduced hydrogen bond formation and increased repulsion with the EG SAM leading to a “clean” EG surface, whereas very strong electrostatic interactions between LPEI and the COOH/COO<sup>-</sup> surface result in large amounts of deposited film on the COOH surface. The selectivity of the LPEI/PAA system was very large and positive at pH 4.8, as shown, indicating a strong correlation between the surface force data and the preferred region of deposition between COOH and EG. Finally, at pH 7.0, the attractive interaction between LPEI and the COO<sup>-</sup> surface drops, presumably due to a loss of electrostatic charge on LPEI at high pH. This results in very small adsorbed amounts on the COOH surface; the EG regions continue to act as a resist, leading to small positive selectivity values at neutral pH.

**3.3. Interactions between the PAH Colloidal Probe and SAM Surfaces as a Function of pH. 3.3.1. PAH Colloidal Probe versus COOH SAM Surface.** Studies of the PAH polyamine gave very different results from the LPEI interactions described above. The force data are shown in Table 3 for the PAH colloid probe on both the COOH and the EG surfaces. Before discussing the data, it is important to address the charged state of the polyamine, PAH, in solution as a function of pH. It is known that the  $pK_a$  of polyamines is generally a decreasing function of degree of ionization.<sup>57</sup> For branched polyethyleneimine, for example, the  $pK_a$  varies from 4.0 to 8.0 depending on the degree of protonation.<sup>58</sup> Although some literature reports give  $pK_a$  values of 9.0 for PAH, degrees

**Table 3. Jump-to-Contact and Pull-Off Force as a Function of pH and Surface Functionality for the PAH Probe ( $R = 3.8 \mu\text{m}$ )**

pH	surface	jump-to-contact force $F$ (nN)	reduced jump-to-contact force $F/R$ (mN/m)	pull-off force $F$ (nN)	reduced pull-off force $F/R$ (mN/m)
2.5	COOH	$0.97 \pm 0.11$	$0.255 \pm 0.029$	$10.8 \pm 0.88$	$2.84 \pm 0.23$
4.8	COOH	$0.01 \pm 0.02$	$0.003 \pm 0.005$	$0.6 \pm 0.09$	$0.16 \pm 0.02$
7.0	COOH	$0.08 \pm 0.06$	$0.021 \pm 0.016$	$1.0 \pm 0.31$	$0.26 \pm 0.08$
2.5	EG	$0.40 \pm 0.07$	$0.105 \pm 0.018$	$1.81 \pm 0.22$	$0.48 \pm 0.06$
4.8	EG	$0.83 \pm 0.04$	$0.218 \pm 0.011$	$2.8 \pm 0.07$	$0.74 \pm 0.02$
7.0	EG	0	0	$1.0 \pm 0.61$	$0.26 \pm 0.16$

of ionization for PAH have been reported to be as low as 70% at pH values of 7.0–7.5.<sup>59</sup> In a different independent study, experimental titration measurements on PAH have been fit to apparent ionization constants which vary with polymer charge density; based on this fit, the degree of ionization of PAH at pH = 5.0 was calculated to be as low as 30%.<sup>60</sup> The reason for the variation of  $pK_a$  with degree of ionization in polyelectrolytes is the difficulty of adding charge incrementally to an already ionized polymer backbone due to effects of charge repulsion. These effects are enhanced for hydrophobic polyelectrolytes for which attractive intrachain interactions bring segments closer together.<sup>57,61</sup> In general, confined films and surface attached primary amino SAMs have also exhibited even lower extents of protonation; the  $pK_a$  of an amino silane SAM measured by force titration is just 3.9.<sup>42</sup>

Force versus separation distance curves of the PAH colloidal probe contacted with the COOH SAM are shown in Figure 8 as a function of pH and summarized in Table 3. At the low pH value of 2.5, strong adhesive interactions take place between the PAH and the COOH surface, reflecting ionic as well as hydrogen-bonding interactions. The PAH is highly protonated at pH 2.5, but the acid surface is also in its protonated form, with a relatively small fraction of ionized COO<sup>-</sup> groups present. The primary amines of PAH act as strong hydrogen bond donors to the carboxylic acid groups, providing opportunity for increased adhesion through hydrogen bonding.

At pH = 4.8, the adhesive interactions of PAH with COOH are significantly reduced to approximately 0.6 nN. Given the fact that the COOH groups are partially ionized at this pH and the PAH is still fairly ionized,<sup>62</sup> one would expect a strong increase in ionic interactions, as was observed for the LPEI probe. The observation of decreased attractive forces is therefore not intuitive. In light of the fact that LPEI, which has a  $pK_a$  value of 5.0, does not exhibit this anomalous behavior, one critical difference in these two systems is likely the difference in segmental arrangements of the two polyamines in solution. As mentioned earlier, PAH has a much more hydrophobic backbone consisting of a vinyl repeat unit, whereas LPEI is hydrophilic, with a secondary amine as part of the main chain. Weak polyelectrolytes have been described as an extended chain of globular spheres in which the globule size, and thus the thickness of the chain, depends on the ionization degree of the polyelectrolyte.<sup>63</sup> The polymer chain conformation, and therefore the exterior surface

(59) Yoshikawa, Y.; Matsuoka, H.; Ise, N. *Br. Polym. J.* **1986**, *18*, 242–246.

(60) Suh, J.; Paik, H.-J.; Hwang, B. K. *Bioorg. Chem.* **1994**, *22*, 318–327.

(61) Chodanowski, P.; Stoll, S. *J. Chem. Phys.* **1999**, *111*, 6069–6081.

(62) Ochiai, H.; Anabuki, Y.; Kojima, O.; Tominaga, K.; Murakami, I. *J. Polym. Sci., Part B: Polym. Phys.* **1990**, *28*, 233.

(63) Grosberg, A. Y.; Khokhlov, A. R. *Statistical Physics of Macromolecules*; AIP Press: New York, 1994.

(57) Sassi, A.; Beltran, S.; Hooper, H.; Blanch, H.; Prausnitz, J.; Siegel, R. *J. Chem. Phys.* **1992**, *97*, 8767–8774.

(58) Nagaya, J.; Homma, M.; Tanioka, A.; Minakata, A. *Biophys. Chem.* **1996**, *60*, 45–51.

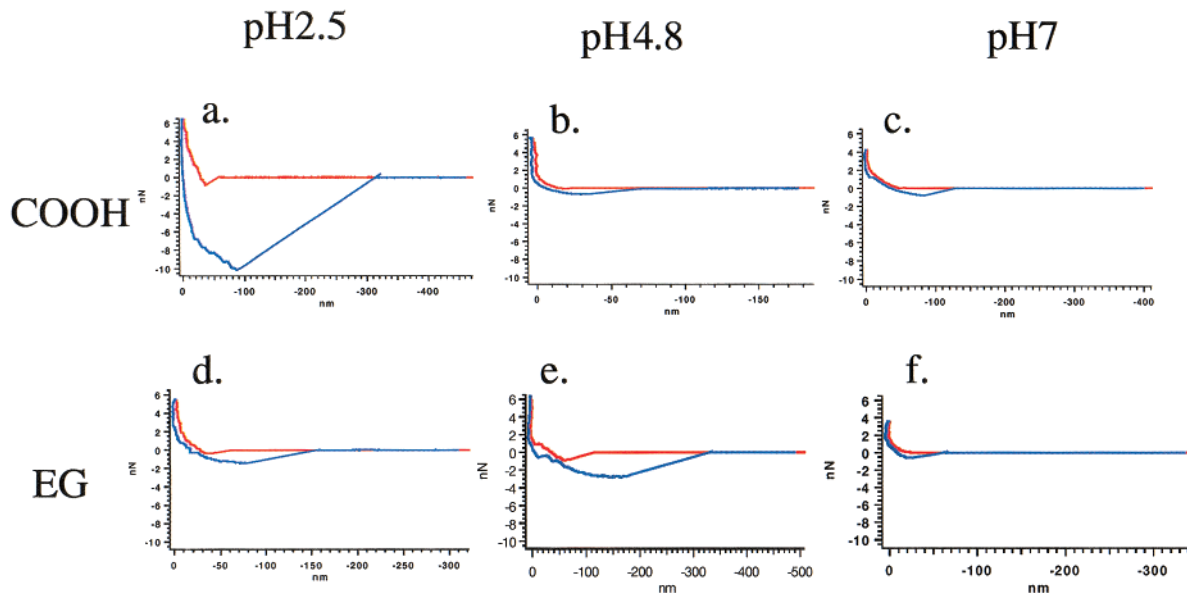


**Figure 8.** Representative in situ force–distance curves of the PAH colloidal probe on the COOH SAM and EG SAM surfaces: (a) on COOH SAM at pH 2.5; (b) on COOH SAM at pH 4.8; (c) on COOH SAM at pH 7.0; (d) on EG SAM at pH 2.5; (e) on EG SAM at pH 4.8; (f) on EG SAM at pH 7.0. (Curves shown are representative samples taken from an ensemble of hundreds of measurements.)

groups of the PAH chain in solution, will vary with decreasing degrees of ionization, with the introduction of more hydrophobic backbone segments at or near the surface at lower degrees of protonation. Conformational changes that occur in PAH at pH 4.8 can result in reduced interactions of the  $\text{COO}^-$  with the amine groups in PAH, in comparison to the more extended, fully hydrated chains at pH 2.5. This proposed model will be addressed in detail in the discussion in section 3.3.3.

The attractive pull-off force remains approximately the same when the pH is increased from 4.8 to 7.0. As the pH is increased to 7.0, the acid groups become very highly ionized ( $\sim 80\%$ ); however, the degree of protonation of PAH is decreased, resulting in little or no net change in the adhesive interaction.

**3.3.2. PAH Colloidal Probe versus EG SAM Surface.** The adhesion of PAH when contacted with EG surfaces is also shown in the force–separation curves of Figure 8. At low pH, the PAH undergoes favorable attractive interactions with the EG surface based on hydrogen bonding similar to that observed in LPEI. The relative size of this force is significantly less than the attractive interaction on the COOH surface at the same pH. However, at pH 4.8 the attractive force between PAH and the EG SAM is noticeably larger and evident in both the jump-to-contact and pull-off force values. The force–separation curve indicates a deep attractive well over a very broad range of distances on pull-off. At this pH, strong secondary interactions take place between PAH and the neutral EG surface. Selective deposition experiments from our earlier report included a study of continuous polyelectrolyte deposited films on a number of different surfaces, including sulfonic and carboxylic acid SAMs and methyl-terminated SAMs.<sup>19</sup> Thicker layers of PAH multilayers adsorbed onto the hydrophobic methyl regions than on either of the acidic surfaces, giving selectivities similar to those on EG versus acid surfaces. These studies indicated the strong role of hydrophobicity in selectivity of PAH on surfaces. Based on these findings and the architectural differences between PAH and LPEI, the interactions are thought to be due to strong hydrophobic interactions between the nonpolar ethylene groups of the EG functionality and the hydrocarbon backbone of PAH;

contributions may also be attributed to the pairing of hydrogen bond donor/acceptor pairs.

Unlike LPEI, PAH can take advantage of both the nonpolar and polar interactions with the EG surface, because it has a hydrophobic region that is decoupled from its polar amino side group. PAH is also less likely to be as hydrated as LPEI, which has a polar heteroatomic backbone. This lower degree of hydration in PAH can reduce the steric and hydration repulsion effects that prevent intimate contact between LPEI and the EG surface at moderate and high pH.<sup>12</sup>

At pH 7, it is likely that the PAH is approaching or perhaps even beyond its true  $pK_a$  value, as discussed above. The pull-off force of PAH on EG decreases to 1.0 nN, a number that is still relatively substantial. The roughly 40–50% decrease in adhesion may be due to the loss of some degree of protonation of the PAH chain and thus the loss of hydrogen bond interactions, which suggests that the adhesion of PAH to the EG surface at this pH is almost completely reliant on hydrophobic interactions alone. An alternate explanation is that the chain conformation of PAH at such high pH approaches that of a collapsed coil, with minimized interactions with both the EG and COOH surfaces.

It appears that at all three pH values, the PAH undergoes measurable attractive interactions with the EG surface; however, these interactions are optimized at pH = 4.8 to yield a strong attractive force.

**3.3.3. Correlation of Adhesion Forces of the PAH Colloidal Probe Tip with Selectivity Data.** A summary of the pull-off force observed in the PAH/SAM system as a function of pH is shown in Figure 9. A strong correlation exists between the magnitude of the pull-off forces and the adsorption selectivity observed with PAH when coadsorbed with the polyanion, PAA, onto COOH/EG patterned surfaces.<sup>19</sup> At low pH (pH = 2.5), PAH/PAA multilayers adsorbed onto both the COOH and EG surfaces, with greater adsorption on the COOH surface. The net positive selectivity based on multilayer film thickness measurements is consistent with the adhesion force differences observed on the COOH versus EG surface at pH 2.5 (see Figure 9). The adsorption data at pH 4.8 indicates much thicker deposition on the EG surface and

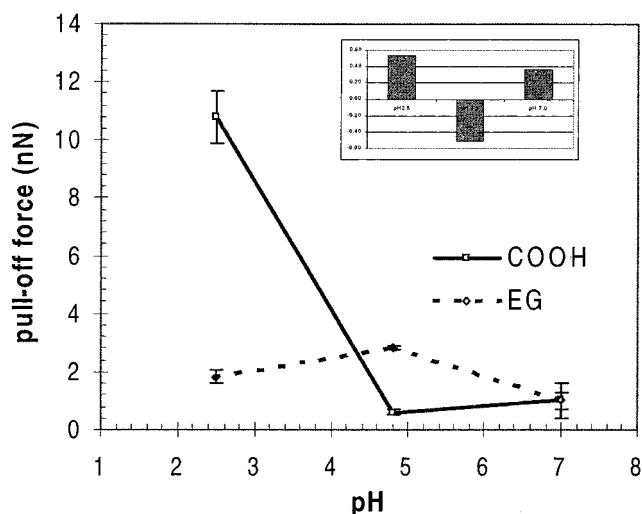


**Figure 9.** Summary of averaged pull-off forces for PAH on the COOH and the EG surfaces. The inset shows the selectivity data from thickness measurement on multilayer films.

a negative selectivity of  $-0.5$  for PAH/PAA film,<sup>19</sup> confirming the pull-off data in Figure 9 as well, which indicates stronger driving forces for adhesion of PAH to the EG surface.

It is apparent from the adsorption data reported previously and the corresponding surface force measurements discussed here that important configurational changes take place with PAH in solution as pH 4.8 is approached. Based on literature references for PAH and other weak polyamines,<sup>58–60,64</sup> the degree of ionization at pH 4.8 may range from 30 to 80%, depending on concentration, molecular weight, and ionic strength. At pH 2.5, PAH is strongly charged and should exist as a highly expanded coil in solution. As the pH is increased from 2.5 to 4.8, it is anticipated that the PAH degree of ionization decreases significantly. It is proposed that with the onset of lower degrees of ionization, hydrophobic association between aliphatic polymer backbone segments is enabled, resulting in the formation of intermolecular clusters or aggregates of hydrophobic segments within the polymer coil. Such a conformational change would create accessible hydrophobic regions of the polymer that can undergo interactions with hydrophobic surfaces. PAH adsorbs strongly to the EG surface, which has both polar and apolar groups, under these conditions. This proposed model is supported by experimental and theoretical studies of weak hydrophobic polyelectrolytes presented by several groups in the past several years. Monte Carlo simulations of hydrophobic polyamines performed by Prausnitz et al.<sup>57</sup> indicate that hydrophobic interactions along the polymer main chain can greatly influence chain conformations. At low pH values, the polymer is treated as an extended coil which contracts with increasing pH as a result of aggregation of hydrophobic units within the chain. This type of change is consistent with the observed change in adsorption behavior and increased hydrophobicity of PAH at pH 4.8. Dobrynin et al.<sup>65</sup> and Chodanowski et al.<sup>61</sup> created models to describe systematic transitions of weak hydrophobic polyelectrolytes with decreased ionization and described the formation of “pearl necklace” conformations consisting of extended chains connected to small globular regions of aggregated segments along the polymer

chain. Finally, the concept of cluster formation between hydrophobic regions of the polymer chain has been used to describe experimental titration data of PAH as well as branched and alkyl-modified polyethyleneimine.<sup>60</sup> Here, as well, the degree of ionization influences the actual  $pK_a$  of the polymer chain, and hydrophobic systems yield more marked deviations from the ideal  $pK_a$  curves. Based on the above discussion, it is proposed that PAH undergoes a conformational transition corresponding to a significant decrease in the degree of ionization of the chain. These conformational changes correspond to clustering and aggregation of hydrophobic regions on the polymer chain; these hydrophobic regions enhance interactions with the EG surface at pH 4.8. It is also anticipated that the effective double-layer electrostatic and hydration repulsion originating from the PAH would be decreased in this case.

It has been suggested that the oligoethylene oxide segment in its amorphous or helical form on gold surfaces generally prevents the deposition of proteins due to the presence of a hydration layer;<sup>12</sup> however, most of the related experiments have focused on protein adsorption, for which the polymer main chain is a more hydrophilic polypeptide backbone. In this study, we use the same EG alkanethiolate SAMs on gold surfaces. Unlike the findings of Grunze et al. with protein adsorption, we find that synthetic polymers with hydrophobic backbones will adsorb to these EG surfaces over specific pH ranges which appear to correspond to a less hydrated state of the polymer chains. The conformation of PAH in solution is also expected to contribute to the shielding of ionic interactions between PAH and the COOH surface at pH 4.8. Conformational changes have been observed in other polyelectrolytes in aqueous solution as a function of pH, the most notable being that of poly(methacrylic acid) (PMAA), which also exhibits a hydrophobic nature due to the presence of the  $\alpha$ -methyl group. Adsorption experiments indicate similar preferred adsorption to the EG surface with poly(methacrylic acid) at low pH,<sup>19</sup> just before the PMAA molecule undergoes a conformational transition at its  $pK_a$ .<sup>66</sup>

Along with the important role of hydrophobic interactions, another possible contributor to the adhesion of PAH on the EG surface at pH 4.8 is hydrogen bonding between the ionized  $NH_3^+$  of PAH and the ether oxygens present in the oligoethylene glycol surface, as discussed earlier. As pH was increased to pH 7.0, PAH became less protonated and exhibited a more collapsed conformation. Therefore, due to less contact with the planar surface, the force decreased from pH 4.8 to 7.0. The net result at pH 7 is that almost equal amounts of deposition occur on both the EG and COOH surfaces, with a small positive selectivity for the COOH surface as reported earlier.<sup>19</sup>

#### 4. Conclusions

Polyamine-modified polystyrene latex colloids were prepared by chemical grafting via electron beam irradiation and characterized extensively using the techniques of XPS, SEM, and fluorescence microscopy. The modified colloidal particles were employed as force probes in the technique of high-resolution force spectroscopy, making it possible to directly measure the intermolecular interactions of different polyamines and functional SAM surfaces in aqueous solution for the first time. The magnitude of adhesion forces of a heteroatomic hydrophilic polyamine, LPEI, and a polyamine with a hydrophobic polymer backbone, PAH, on COOH SAM and EG SAM surfaces

(64) Ochiai, H.; Anabuki, Y.; Kojima, O.; Tominaga, K.; Murakami, I. *J. Polym. Sci., Part B: Polym. Phys.* **1990**, *28*, 233–240.

(65) Dobrynin, A. V.; Rubinstein, M.; Obukhov, S. P. *Macromolecules* **1996**, *29*, 2974.

(66) Bloys van Treslong, C. J. *Recl. J. R. Neth. Chem. Soc.* **1978**, *97*, 13–21.

was measured at different pH levels. We found that there was a direct correlation between the molecular-level polyamine-SAM interaction forces and previously reported multilayer adsorption selectivity data of these two very different polyamines. The results confirm that the architecture of the polyion chain, as well as its charge density, can greatly influence the amount of polymer deposited on charged surfaces and on neutral EG surfaces.

The adhesion of the more hydrated LPEI on the COOH surface was optimized by ionic attractions at the moderate pH level of 4.8 but weakened at low pH and high pH levels because of reduced ionization of the COOH and LPEI systems, respectively. Repulsion dominated the interactions between LPEI and the EG surface at moderate to high pH ranges, but it was found that hydrogen bonding can induce minimal adhesion of LPEI on the EG surface at the low pH level of 2.5.

Surprisingly, it was shown that favorable adhesive interactions could take place between the hydrophobic PAH polyamine and the EG surface. This observation confirms earlier reports of selective deposition of polyelectrolyte multilayers, in which LPEI-based multilayers deposit preferentially on the COOH surface, but PAH-based multilayer films deposit preferentially on the EG surface. Hydrophobic interactions and hydrogen bonding contribute to the adhesion of the polyamine to the EG surface; the adhesion is optimized at pH 4.8. This result illustrates the rather counterintuitive concept that oligoethylene oxide usually used as resists to protein deposition can actually become regions of preferred adsorption via hydrophobic and other secondary interactions. With regard to the COOH SAM surface, hydrogen bonding and ionic interactions between the primary amine groups of PAH and COOH are dominant at low pH. Weakened ionic attractions induce a small amount of adhesion of the PAH polymer to the COOH surface at moderate and high pH levels and are thought to decrease due to changes in the conformation of PAH from an

expanded state to a partially collapsed coil with increasing pH. Ongoing light scattering experiments confirm the presence of a conformation transition in PAH, and will be reported separately.

Future work will be carried out using molecular-level theoretical simulations to quantitatively predict and deconvolute the constituent components of the total polyamine-SAM intermolecular interaction. Hence, the HRFS data obtained here provide us with a unique opportunity to directly quantify the roles of each of the different forces involved in selective multilayer deposition and nanostructure formation. We can apply our molecular-level understanding of these surface interactions to template the formation of lateral multicomponent multilayer films.<sup>21</sup> This information will also contribute to the understanding of interactions between synthetic polymers and biopolymers, such as proteins and hydrated EO surfaces.

**Acknowledgment.** Professor Edward Merrill in the department of Chemical Engineering at MIT is thanked for the useful discussion about surface grafting with electron beam irradiation, and Mr. Kenneth Wright in the High Voltage Laboratory of MIT is thanked for performing the electron beam irradiation. Solar Olugebefola in the department of Material Science and Engineering is thanked for the demonstration of gluing particles on the AFM cantilever when this study was started. Joonil Seog in the Ortiz research group is thanked for supplying the gold-coated AFM cantilever for control experiments. Thanks to Dr. Dave Lynn who helped using the zeta potential analyzer, and thanks to Elizabeth Shaw at CMSE of MIT who helped using XPS. Funding for this work was provided by the Office of Naval Research-Polymer Program and by the MIT MRSEC (NSF) grant DMR-9400334.

LA010832Q